Progress on Characterization with Integrated Test Structures of Dielectric and Superconducting Films for SIS Mixer Circuits

D. M. Lea and A. W. Lichtenberger

Applied Electrophysics Laboratories
Department of Electrical Engineering
University of Virginia, Charlottesville, VA 22903 USA

Abstract

The growing use of superconductor-insulator-superconductor (SIS) mixers at both millimeter and submillimeter wavelengths has been accompanied by an increased reliance on integrated tuning and coupling elements. These planar structures, fabricated on the same chips as Nb/Al-AlO_x/Nb SIS junctions, can be used as either a complement or alternative to mechanically adjustable waveguide backshorts. For optimal performance, designs of these structures must be based on accurate predictions of the following crucial film parameters: (1) dielectric constants ε_r of the oxides used in the tuning elements, (2) magnetic penetration depth λ of the Nb films, (3) specific capacitance C_s of the SIS trilayer, and (4) critical current density J_c of the SIS trilayer. Here we report on measurements of these quantities at T = 4.2 K using test structures that were fabricated by the same process which we use for Nb/Al-AlO_x/Nb mixer circuits.

1. Introduction

As the operating frequencies of Nb/Al-AlO_x/Nb superconductor-insulator-superconductor (SIS) tunnel junction mixers have increased, a greater emphasis has been placed on the use of integrated tuning and coupling structures. The need for tuning arises from the capacitance of the junctions, which creates a parasitic susceptance that increases linearly with frequency, degrading mixer performance [1]. Consequently, many SIS receiver designs incorporate some method of inductive tuning to substantially lower this parallel susceptance over the desired range of operating frequency. Adjustable waveguide short circuits continue to play a large role as tuning structures at both millimeter and submillimeter wavelengths, but it has become common to combine their use with that of on-chip structures [2-4]. This approach increases mixer bandwidth and relaxes strict tolerances on waveguide shorts. Some groups have taken the reliance on integrated structures a step further with "fixed-tuned" mixer designs, in which waveguide shorts do not require adjustment [5-7]. Still others have chosen to completely avoid the machining and reliability problems associated with the decreasing waveguide and backshort dimensions needed for increasing frequencies. Instead, they rely on quasi-optical techniques (lenses and antennas) to couple radiation to the junctions. (Several references concerning quasi-optical SIS receivers may be found in [8].)

In all of these designs, tuning or coupling structures are used which are planar and can be fabricated on the same substrates as the junctions. Although these integrated structures have already proven quite successful, their designs would improve if the most important electromagnetic properties of the constituent films (magnetic penetration depth, trilayer specific capacitance, and dielectric constants) could be predicted with greater accuracy. Often, mixer designers rely on values for these properties taken either from the literature or from their own measurements on a small set of films with little variation in thickness or deposition parameters. Such values may not reflect accurately the characteristics that the films in a mixer circuit will have; thus, they do not permit direct correlation of film characteristics with mixer performance.

The work described in this paper was undertaken to permit better measurements and predictions of the film characteristics just mentioned. We have developed a systematic approach to measuring the main quantities of interest using structures which can be fabricated on the same wafers as our Nb/Al-AlO_x/Nb mixer circuits, with no additional processing steps. A photomask set was designed which consists entirely of a variety of geometries of these structures. We are presently compiling an extensive set of measurements on structures fabricated with this mask set so that we can gain a thorough understanding of geometrical factors affecting the results, allowing us to minimize measurement errors. We have also selected a subset of these structures, occupying a compact region, for inclusion in our next mixer mask set. In the following sections, we discuss the design of these structures and appropriate test fixtures, as well as the results of our measurements to date.

2. General Measurement Strategy

Since one of the main objectives is improved tuning of the capacitance of Nb/Al-AlO_x/Nb junctions in mixers, we consider first a method for measuring specific capacitance C_s (capacitance per unit area) of these trilayers. C_s should obey the simple parallel plate formula $C_s = \varepsilon_r\varepsilon_0/d$, but it is impossible to measure directly either the relative dielectric constant ε_r or the thickness d of the AlO_x layer with sufficient accuracy. This layer is only on the order of tens of angstroms in thickness; moreover, it is covered by the Nb counter electrode layer (M2). We must instead rely on an indirect technique to measure C_s; we chose to measure it through observation of Fiske resonances [9-12] in long SIS junctions, primarily because it will be quite simple to incorporate one or more long junctions into the testing regions of future mixer mask sets. Although trilayer films with high values of critical current density J_c (10^4 A/cm^2 or greater) are being included in the study, we do not expect heating effects to introduce errors into our measurements, since the first few Fiske resonances produce relatively low currents even in junctions with high J_c.

As will be discussed further in Section 3.C., the extraction of an accurate value of C_s from Fiske resonance measurements requires that two other quantities be measured as well: (1) the London penetration depth λ_L of the Nb films used, and (2) the relative dielectric constant ε_r of the insulator (in our case, either SiO or Nb_2O_5) which surrounds the junction to isolate the base electrode (M1) from the interconnect wiring (M3). These quantities are also of interest due to their importance to the proper design of tuning structures once C_s is known. The remaining quantity we wished to measure is J_c, which is best measured using junctions smaller than the ones used for observation of Fiske resonances. Thus, in all, our characterization scheme includes structures for measurement of four film properties.

In keeping with our desire to rely on structures that will be relatively simple to include on mixer circuit wafers, we chose to use thin-film capacitors for measurements of ε_r of SiO and Nb_2O_5 films, and microstrip resonators to measure λ_L of Nb films. We designed them so that, like the SIS junctions used for measuring C_s and J_c, they can be fabricated concurrently with a mixer circuit. Generic examples of the test structures we designed, and a process for fabricating them concurrently, are depicted in Fig. 1. Our general process [13] is based on the SNEP process [14], but the structures should be realizable with any planar SIS junction process that uses an interconnect wiring layer. The microstrip resonators use SiO or Nb_2O_5 as the dielectric; thus, determining a value of λ_L (which will be discussed in Section III.B.) requires an accurate value of ε_r of those oxides. This does not pose a problem; the thin-film capacitor method of measuring ε_r is independent of λ_L, depending only on the more easily measured quantities of area and dielectric thickness. To allow estimation of error in our ε_r measurements, we included capacitors of different areas in our mask design, and have used different oxide thicknesses in processing different wafers.

This approach, using different geometries, oxides, and oxide thicknesses to confirm measurements, was applied to the other types of structures as well. For example, like the capacitors, half

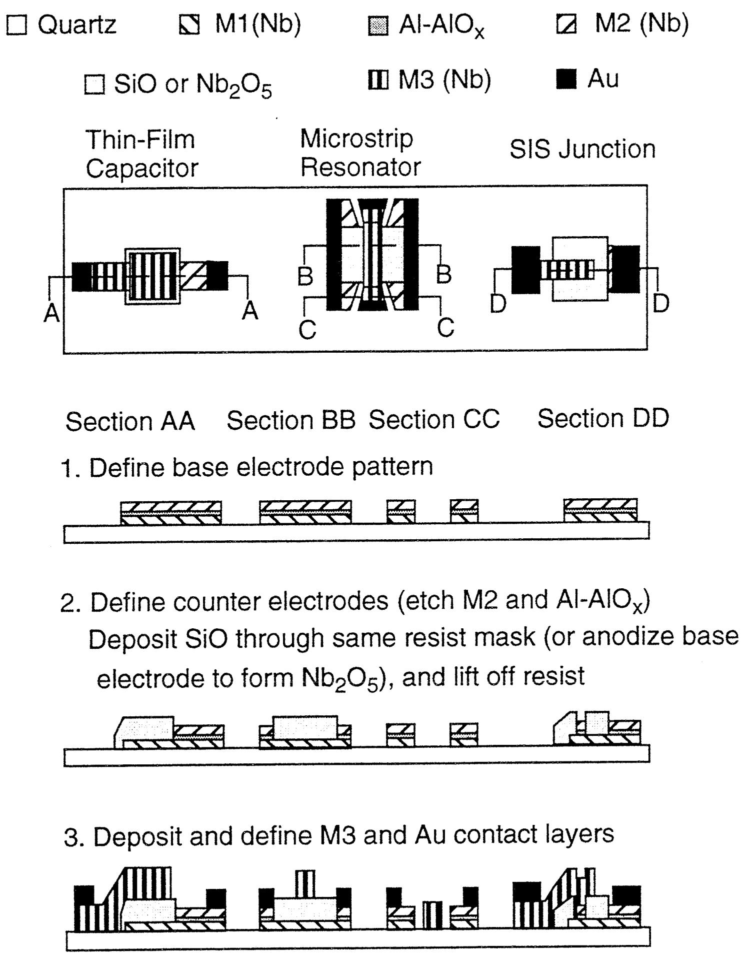

Fig. 1. Top views of completed test structures, and section views at various stages of fabrication process. Structures are not drawn to scale. In regions where M2 is directly contacted by Au, we may consider M2 and M1 to be a single layer because the SIS junction between them has sufficient area to create a short whose critical current will not be exceeded.

of the microstrip resonators and SIS junctions on the mask set use SiO as a dielectric, while the other half use Nb_2O_5. The general measurement strategy is as follows:

(1) Obtain ε_r of SiO and Nb_2O_5 from thin-film capacitor measurements.

(2) Use values of ε_r in obtaining λ_L of Nb from S-parameter measurements of microstrip resonators.

(3) Use values of ε_r and λ_L in obtaining C_s of trilayer from observation of Fiske resonances in long SIS junctions.

(4) (Independent of first three steps) Obtain J_c of trilayer from dc I-V measurements of smaller SIS junctions.

3. Design Details and Measurement Procedures

A. Thin-Film Capacitors

Any planar SIS junction fabrication process featuring an M3 layer lends itself to simple fabrication of capacitors using M1 and M3 as the electrodes and the junction insulation layer as the dielectric. Examining Sections AA and DD of Fig.1, we see that this approach can indeed be applied to our process. Thus, Nb_2O_5 capacitors can be made on one half of each wafer, concurrently with junctions defined by SNAP; SiO capacitors can be made on the other half, concurrently with junctions defined by SNEP. Two different areas, 1.00 mm^2 and 2.00 mm^2, were chosen. Based on calculations using those areas, the dielectric thicknesses typically used in SIS mixer circuits, and values of ε_r (29 for Nb_2O_5 and 5.7 for SiO) taken from the literature [15, 16], the capacitance values were expected to be on the order of 1 nF for the Nb_2O_5 capacitors and 100 pF for the SiO capacitors. The capacitance of any parallel-plate structure is affected at least slightly by field fringing at its edges, but calculations based on [17, 18] indicated that field fringing would add less than 1% to the capacitance of our structures. So that we could verify that the field fringing is indeed negligible in practice, we chose to include circular and square capacitor geometries possessing the same areas.

Fig. 2 shows the design of a brass fixture for holding and contacting the capacitors in liquid helium. Capacitor chips are mounted in the fixture using Apiezon H vacuum grease [19], allowing easy removal after testing. Wire bonding is used to make contact from the probes to the Au pads. Two identical fixtures were made; our helium dip probe was designed such that the two fixtures are inserted together, each connected to its own pair of 50 Ω stainless steel coaxial cables, as shown in Fig. 2. One purpose of this arrangement was to allow one fixture to be used as a "dummy" (with no chip mounted), so that line-to-line capacitance could be determined and subtracted out during each measurement. Subsequently, since the line-to-line capacitance has remained very consistent, the two-fixture arrangement has been exploited to measure two capacitor chips during each cycle into liquid He.

B. Microstrip Resonators

Returning to Fig. 1, we can see that the same three layers used to form thin-film capacitors are also well-suited for forming microstrip transmission lines, with M1 as the ground plane and M3 as the strip conductor. For all of our microstrip lines, the ratio w/d (w is the width of strip conductor, d is the dielectric thickness) is greater than 50, allowing us to use Swihart's formula [20] for

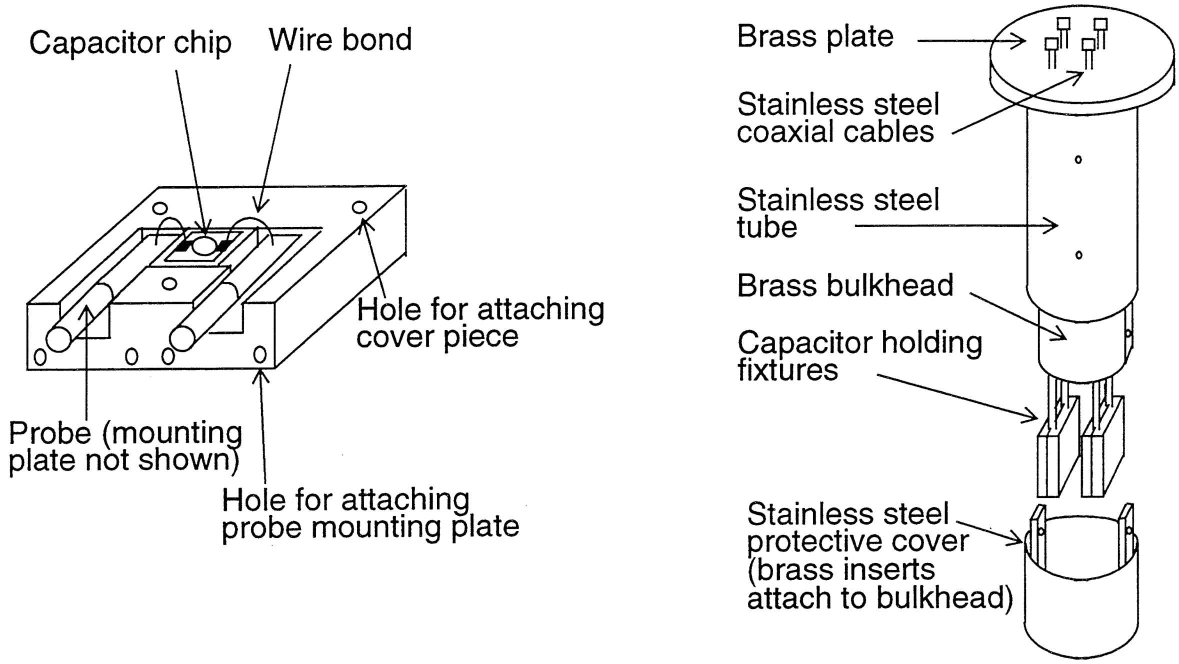

Fig. 2. Capacitor holding fixture (cover piece not shown), and assembly of dip probe for insertion into liquid He.

the relationship between λ_L and the phase velocity v_{ph}

$$v_{ph} = \frac{c}{\sqrt{\varepsilon_r \cdot \left[1 + \left(\frac{\lambda_{Lg}}{d}\right) \cdot \coth\left(\frac{t_g}{\lambda_{Lg}}\right) + \left(\frac{\lambda_{Ls}}{d}\right) \cdot \coth\left(\frac{t_s}{\lambda_{Ls}}\right)\right]}}$$

(c = velocity of light in a vacuum; d = dielectric thickness; t = metal thickness; subscripts g and s refer to ground plane and strip conductor)

without having to include Chang's correction factors [21]. The measurement of the resonant frequencies of microstrip lines is used to determine their values of v_{ph} [22]. We have chosen microstrip geometries which possess values of characteristic impedance Z_c on the order of 1 Ω; thus, coupling these lines to 50 Ω coaxial lines at both ends results in resonances which appear in measurements of the scattering parameter S_{21} as a function of frequency. Seven resonator lengths ranging from 8 mm to 20 mm in increments of 2 mm are included on the mask set. Calculations indicated that the fundamental resonant frequencies of the different resonators would range from several hundred MHz, for the longest Nb_2O_5 resonators, to several GHz, for the shortest SiO resonators.

Consideration of the coupling to the cables led to two features of our design. The first is the use of a tapered coplanar waveguide section, visible in Fig. 3, at each end of the microstrip line. It was designed to have Z_c = 50 Ω, so that the large discontinuity in Z_c occurs at the end of the microstrip. Therefore, the exact length of the resonant transmission line is clearly defined; this would not be the case if wire bonds were made directly to the microstrip. The center conductor, made from M3, spreads out from the 50 μm width of the microstrip conductor to a width of 200 μm at the end to provide more room for a wire bond. The other end of the bond wire could be attached *directly* to a Type K Connector [23] which in turn connects to the 50 Ω cable; however, a better approach is to use a section of 50 Ω Cuflon [24] microstrip between the resonator chip and the K Connector, as shown in Fig. 3. This feature shifts the location of the repeated bonding and bond breaking required as different resonators are tested. As a result, these processes take place on the Cuflon and resonator chips, so that the connection to the delicate K Connector pin can be a solder connection that only has to be made once. Due to the low ε_r of teflon, the amount of dispersion introduced by the Cuflon sections is negligible over the frequency range (500 MHz to 20 GHz) used in the measurements.

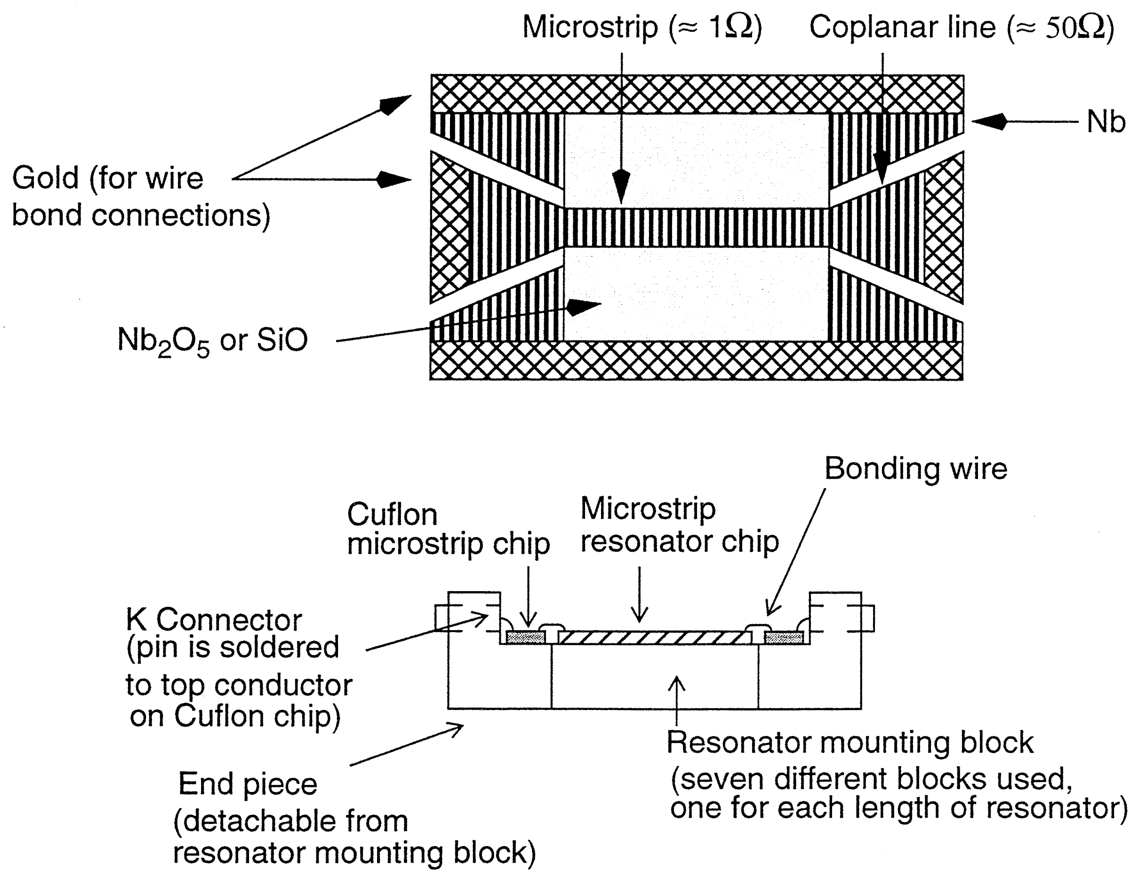

Fig. 3. Microstrip resonator chip and resonator test fixture assembly (wire bonds for ground connections not shown)

The dip probe pictured in Fig. 2 was designed for resonator as well as capacitor measurements. At one end, the resonator holding fixture attaches directly to the end of one of the 50 Ω cables. The other end of the fixture faces away from the cables, so we connect to it using a cable with a U-shaped bend. We can then insert the dip probe into a liquid He dewar, connect the probe to an HP8720 network analyzer [25], and measure S_{21} as a function of frequency.

C. SIS Junctions

The SIS junctions on this mask set were designed to be testable using our existing I-V test fixture and probe. There are fifteen junctions of different geometries on the SiO-insulated half of the mask set, and the same fifteen geometries are repeated on the Nb_2O_5-insulated half. Twelve of the geometries are devoted to the observation of Fiske resonances. Lee [11,12] has demonstrated that because the electromagnetic wave created by the ac Josephson effect is not strictly confined to the region below M2, the voltage spacing between Fiske resonances depends not only on C_s, but also to some extent on (1) the thickness and ε_r of the junction insulation regions overlapped by M3 on either side of the junctions, and (2) the magnetic penetration depth of the Nb layers. To further investigate these effects and obtain more precise values of C_s, we used a variety of values of junction width, junction length, and M3 overlap width in our mask design, and have used several different thicknesses of each junction insulation oxide in our processing.

The three remaining junctions on each half are for measuring J_c; they are circular, with diameters of 4, 6, and 8 μm. These sizes were chosen to be large enough that uncertainty in area due to processing variations is only a small percentage of the area, yet small enough that current distribution is still nearly uniform even when J_c is between 10^4 and 10^5 A/cm^2 [26]. The uniform current distribution allows us to simply divide I_c by the junction area A in order to determine J_c.

4. Measurement Results

At this time, approximately forty wafers have been processed using the characterization mask set; roughly half of those wafers have yielded meaningful measurements. We begin our discussion by considering measurement results for the planar capacitors with Nb_2O_5 as the dielectric. The first approximately thirty wafers were Nb/Al-AlO_x/Nb trilayers with relatively thin (~ 500 Å) counter electrode (M2) layers. As a result, the anodized dielectric layer in the planar capacitors always contained a layer of AlO_x in addition to the Nb_2O_5, making the calculation of ε_r less certain. As indicated by the left two-thirds of Fig. 4, most of the measurements on these mixed-dielectric capacitors yielded results of $\varepsilon_r = 41 \pm 10\%$. These results were surprising when compared to the

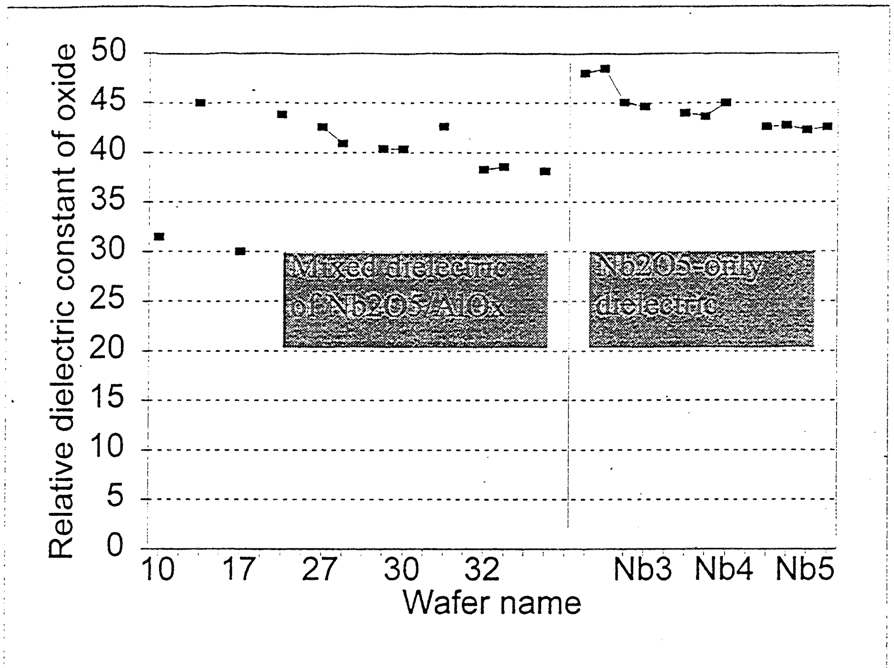

Fig. 4. Measured values of relative dielectric constant ε_r for Nb_2O_5 capacitors.

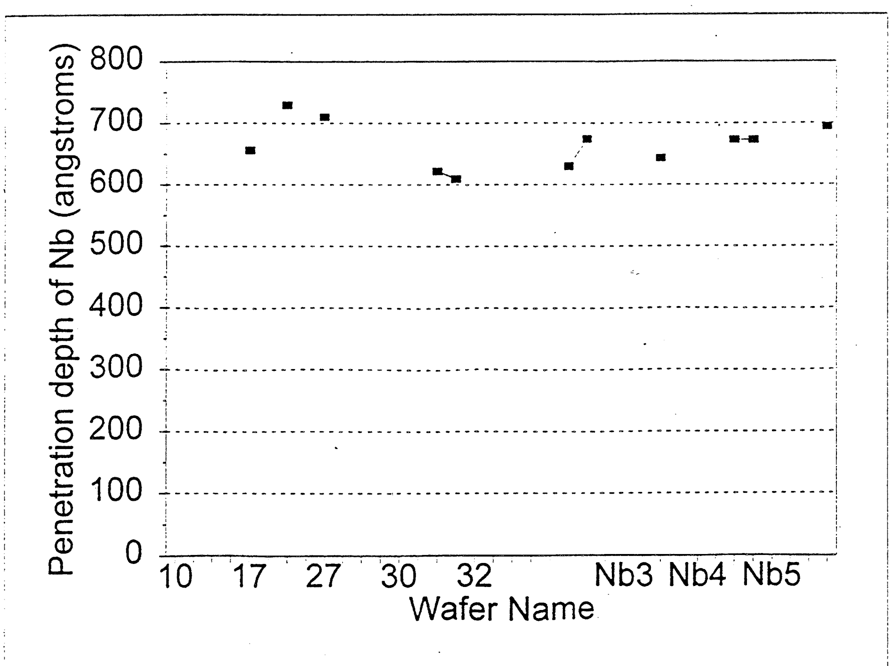

Fig. 5. Measured values of magnetic penetration depth λ for Nb films.

result ε_r = 29 obtained in [15]. Thus, it seemed important to us to fabricate some capacitors in which the dielectric consisted only of Nb_2O_5, as opposed to the mixed-dielectric structure, to obtain more definitive measurements. Consequently, we processed several trilayers with a barrier layer consisting of only Al (no AlO_x), and having a thick (~ 1500 Å) M2 layer, which enabled us to create capacitors by only anodizing part of the way through M2. (These wafers were given the prefix "Nb" before their numerical designation: Nb1, Nb2, etc.)

Results from the Nb_2O_5-only capacitors are shown in the rightmost third of Fig. 4, and fall within the range er = 44 ± 10%. Since AlO_x films typically have an ε_r of about 10, it is logical that the Nb_2O_5-only capacitors would yield a higher value for ε_r than that of the mixed-dielectric capacitors. This value of ε_r for the Nb_2O_5-only capacitors is a full 50% higher than the value obtained in [15], but is in good agreement with many values in the electrochemistry literature [27, 28]. We have begun some experiments attempting to link ε_r of Nb_2O_5 to anodization parameters (e.g., current density, hold time), which may at least partially explain the differences in values obtained. Another plausible explanation is that differences in Nb films (such as different values in film stress) may lead to different characteristics in the oxide films that result when the Nb is anodized.

Our measurements thus far of ε_r of SiO indicate that ε_r = 5.7 ± 10%, which is within our expectations based on [16].

As for the magnetic penetration depth measurements, Fig. 5 indicates a range for λ of 680 Å ± 10%. This value is 20% lower than the result obtained in [15], and may be a reflection of high-quality Nb films due to our efforts to optimize the stress levels of our sputtered Nb films. Further experiments investigating λas a function of our sputtering conditions are in order.

Because our measured values of ε_r for Nb_2O_5 and λ for Nb are significantly different from those appearing previously in the superconductivity literature, we desire to confirm them with more data before attempting to apply them to other calculations. Therefore, it would be premature to try to use them to calculate definitive values for C_s from the Fiske resonance measurements that we have performed. However, we can note that we have observed the expected trend of increasing C_s as Jc increased from roughly 1 x 10^2 to 5 x 10^3 A/cm^2 on the wafers we have tested thus far. The next set of wafers to be processed and tested are ones with J_c on the order of 10^4 A/cm^2; we expect the trend of increasing C_s to continue. The task will then be to develop, based on all of the data obtained, an empirical relationship between C_s and J_c applying to a range of Jc of over two orders of magnitude.

5. Conclusion

We have presented motivation and a strategy for characterization of several key electromagnetic properties of Nb/Al-AlO_x/Nb trilayer films, along with designs of integrated structures and test fixtures for performing the measurements. The ongoing film study using these integrated structures, as well as the inclusion of a subset of the structures in future mixer mask sets, should lead to improved SIS mixer designs.

Acknowledgment

The authors wish to thank several members of the National Radio Astronomy Observatory (NRAO) Central Development Laboratory: A. Kerr, S.-K. Pan, and R. Bradley for assistance in the design of test structures and fixtures, and G. Taylor, W. Lakatosh, N. Horner, and F. Johnson for assistance in the fabrication and assembly of the test fixtures.

This research was supported by a NASA GSRP fellowship, NGT-50820.

References

[1] J. R. Tucker and M. J. Feldman, "Quantum detection at millimeter wavelengths," *Rev. Mod. Phys.*, vol. 57, pp. 1055-1113, Oct. 1985.

[2] A.R. Kerr, S.-K. Pan, and M. J. Feldman, "Integrated tuning elements for SIS mixers," *Int. J. IR MM Waves*, vol. 9, pp. 203-212, Feb. 1988.

[3] M. M. T. M. Dierichs *et al.*, "Evaluation of integrated tuning elements with SIS devices," *IEEE Trans. Microwave Theory Tech.*, vol. 41, pp. 605-608, Apr. 1993.

[4] M. Salez, P. Febvre, W. R. McGrath, B. Bumble, and H. G. LeDuc, "An SIS waveguide heterodyne receiver for 600 GHz - 635 GHz," *Int. J. IR MM Waves*, vol. 15, pp. 349-368, Feb. 1994.

[5] A. R. Kerr and S.-K. Pan, "Some recent developments in the design of SIS mixers," *Int. J. IR MM Waves*, vol. 11, pp. 1169-1187, Nov. 1990.

[6] D. Winkler *et al.*, "A full-band waveguide SIS receiver with integrated tuning for 75-110 GHz," *IEEE Trans. Magn.*, vol. 27, pp. 2634-2637, Mar. 1991.

[7] A. R. Kerr, S.-K. Pan, A.W. Lichtenberger, and D.M. Lea, "Progress on tunerless SIS mixers

for the 200-300 GHz band," *IEEE Microwave and Guided Wave Lett.*, vol. 2, pp. 454-456, Nov. 1992.

[8] J. Zmuidzinas, H. G. LeDuc, J. A. Stern, and S.R. Cypher, "Two-junction tuning circuits for submillimeter SIS mixers," *IEEE Trans. Microwave Theory Tech.*, vol. 42, pp. 698-706, Apr. 1994.

[9] M. D. Fiske, "Temperature and magnetic field dependences of the Josephson tunneling current," *Rev. Mod. Phys.*, vol. 36, pp. 221-222, Jan. 1964.

[10] R. E. Eck, D. J. Scalapino, and B. N. Taylor, "Self-detection of the ac Josephson current," *Phys. Rev. Lett.*, vol. 13, pp. 15-18, July 1964.

[11] G. S. Lee, "Analysis of linear resonances in modern Josephson junction geometries," *IEEE Trans. Appl. Supercond.*, vol. 1, pp. 121-125, Sept. 1991.

[12] G. S. Lee and A. T. Barfknecht, "Geometric and material dispersion in Josephson transmission lines," *IEEE Trans. Appl. Supercond.*, vol. 2, pp. 67-73, June 1992.

[13] A. W. Lichtenberger, D. M. Lea, R. J. Mattauch, and F. L. Lloyd, "Nb/Al-Al_2O_3/Nb junctions with inductive tuning elements for a very low noise 205-250 GHz receiver," *IEEE Trans. Microwave Theory Tech.*, vol. 40, pp. 816-819, May 1992.

[14] M. Gurvitch, M. A. Washington, and H. A. Huggins, "High quality refractory Josephson tunnel junctions utilizing thin aluminum layers," *Appl. Phys. Lett.*, vol. 42, pp. 472-474, Mar. 1983.

[15] W. H. Henkels and C. J. Kircher, "Penetration depth measurements on type II superconducting films," *IEEE Trans. Magn.*, vol. 13, pp. 63-66, Jan. 1977.

[16] H. K. Olsson, "Dielectric constant of evaporated SiO at frequencies between 13 and 103 GHz," *IEEE Trans. Magn.*, vol. 25, pp. 1115-1118, Mar. 1989.

[17] W. C. Chew and J. A. Kong, "Effects of fringing fields on the capacitance of circular microstrip disk," *IEEE Trans. Microwave Theory Tech.*, vol. 28, pp. 98-103, Feb. 1980.

[18] H. A. Wheeler, "A simple formula for the capacitance of a disc on dielectric on a plane," *IEEE Trans. Microwave Theory Tech.*, vol. 30, pp. 2050-2054, Nov. 1982.

[19] Apiezon Products Limited, London, England.

[20] J. C. Swihart, "Field solution for a thin-film superconducting strip transmission line," *J. Appl. Phys.*, vol. 32, pp. 461-469, Mar. 1961.

[21] W. H. Chang, "The inductance of a superconducting strip transmission line," *J. Appl. Phys.*, vol. 50, pp. 8129-8134, Dec. 1979.

[22] B. W. Langley, S. M. Anlage, R. F. W. Pease, and M. R. Beasley, "Magnetic penetration depth measurements of superconducting thin films by a microstrip resonator technique," *Rev. Sci.*

Instrum., vol. 62, pp. 1801-1812, July 1991.

[23] Wiltron Company, Morgan Hill, CA.

[24] 3M Company, St. Paul, MN.

[25] Hewlett-Packard, Santa Clara, CA.

[26] I. Taguchi and H. Yoshioka, "Properties of superconducting point contacts," *J. Phys. Soc. Japan*, vol. 29, pp. 371-379, Aug. 1970.

[27] L. Young, "Anodic oxide films on niobium: thickness, dielectric constant, dispersion, reflection minima, formation field strength, and surface area," *Can. J. Chem.*, vol. 38, pp. 1141-1147, 1960.

[28] F. Di Quarto, S. Piazza, and C. Sunseri, "Amorphous semiconductor-electrolyte junction. Impedance study on the a-Nb_2O_5-electrolyte junction," *Electrochimica Acta*, vol. 35, no. 1, pp. 99-107, 1990.